JAMECH
Vol. 45, No. 1, Sep. 2014. pp 35-45

Numerical and Experimental Analysis and Optimization of Process Parameters of AA1050 Incremental Sheet Forming

Hosein Mohammadi [1*], Masoud Sharififar [2], Ali Asghar Ataee [3]

1. MS Graduate, Department of Mechanical Engineering, University of Tehran, Tehran, Iran

2. Department of Metallurgy and Material Engineering, Malek-Ashtar University of Technology, Tehran, Iran

3. Assistant Professor, School of Mechanical Engineering, University of Tehran, Tehran, Iran

Received 21 August 2014; Accepted 2 September 2014

Abstract

The incremental sheet metal forming (ISMF) process is a new and flexible method that is well suited for small batch production or prototyping. This paper studies the use of the finite element method in the incremental forming process of AA1050 sheets to investigate the influence of tool diameter, vertical step size, and friction coefficient on forming force, spring-back, and thickness distribution. A comparison between numerical and experimental results is made to assess the suitability of the model. An approach for the optimal process factors in the incremental sheet metal forming was proposed, which integrates a finite element simulation technique, artificial neural network, and genetic algorithm. This approach is incorporated to suggest a model for process factors in terms of friction coefficient (μ), vertical step size (S) and tool diameter (D). It is found that the friction coefficient decreases spring-back value whereas vertical step size results vertical force increase and minimum thickness decrease. Tool diameter increases forming force and spring-back values.

Keywords: *finite element method, genetic algorithm, incremental sheet metal forming, neural network.*

1. Introduction

Incremental sheet metal forming (ISMF) is a sheet metal forming technique where a sheet is formed into the final workpiece by a series of small incremental deformations. This method is based on the forming of the metal sheet by means of a Computer Numerical Control (CNC) machine that plastically deforms the blank to the desired shape. The tool trajectory is directly taken from the CAD file of the part to be formed. Regarding the concept of such technology, a wide range of 3D shapes can be formed with correct definition of the forming tool path controlled by a CNC machine. ISMF includes two specific types of incremental forming: single point incremental forming (SPIF) and two point incremental forming (TPIF). In SPIF, a sheet is clamped around its edges and deformed by a simple forming tool (generally of hemispherical shape) that presses on one side of the sheet and moves around

* Corresponding Author. Tel.: + 989132338463
Email Address: h_mohammadin@ut.ac.ir

from a proper forming tool path, whereas in TPIF the sheet is formed against a die or a second mobile tool [1]. The process can offer rapid prototyping advantages for sheet metal parts that are made directly from a 3D CAD model to finished product without the conventional intermediate stage of tool design and manufacture. The idea of incremental sheet metal forming with a single point tool, called 'dieless forming' was patented by Leszak in 1967 [2]. SPIF has been investigated by many researchers, who have underlined its great flexibility due to the absence of specific dies. Micari et al. discussed several methods to improve SPIF capability and concluded that tool path optimization approaches are the most promising [3]. Kim and Park investigated the effect of process parameters on formability and found that a small amount of friction at the tool/sheet interface helps to improve formability [4]. The formability also increased as the feed rate decreased. Durante et al. found that the forming force tends to decrease with tool rotation speed in the incremental forming process of AA7075-T0 sheets [5]. Petek et al. investigated the effect of SPIF process parameters on deformation and forming force, and reported that with an increase in tool diameter and vertical step size, the forming force increases [6]. Duflou et al. investigated the effect of tool diameter, vertical depth increment, thickness of sheet, and wall angle on the forming force of Al3003-O sheets [7]. The reported results indicate that the magnitude of force increases with an increase of tool diameter, depth of the vertical step, and sheet thickness. As the part wall becomes steeper, the magnitude of the force needed to form it also gradually increases. Dejardin et al. demonstrated the accuracy and reliability of 3D finite element simulation of the process [1]. It has been demonstrated through experiments and finite element analyses that spring-back can be accurately predicted from numerical simulations. Henrard et al. studied the accuracy of finite element simulations in predicting the tool force that would occur during the SPIF process [8]. Their study showed that three factors have an influence on force prediction: the type of finite element, the constitutive law, and the identification procedure for the material parameters. Cerro et al. also developed a finite element model to predict the behaviour of the AA1050 sheet during the forming process [9].

In some metal forming processes, researchers combined artificial neural network (ANN) and genetic algorithm (GA) to investigate the relationship between control factors of the forming process and to optimize of them. Sanjari et al. [10] employed the artificial neural network and genetic algorithm method to optimize radial force and strain inhomogeneity in the radial forging process. Yu et al. [11] also developed an integrated approach using an FEM equivalent model, artificial neural networks, and genetic algorithms for optimum path design of press bend forming.

Process factors optimization in ISMF has not been studied, and is essential for producing components with the desired properties, highest quality, and lowest cost. These optimum values, for example, can lead to the selection of cheaper machine tools, prevention of sheet failure in high forces, and an improvement of geometry and shape of the final part. In this study three important factors including friction coefficient, tool diameter, and vertical step size have been optimized to attain minimum values of spring-back and vertical force, and the maximum value of the minimum thickness of the sheet.

2. Methods

The material used in this study was a 1050 aluminium alloy. First the material was annealed at 350°C for 60 min to form an isotropic structure [12]. Then mechanical characterization was carried out by means of tensile tests with a fully automated mechanical test machine (SANTAM).

To investigate the isotropy of the material, tensile tests were performed in rolling direction (RD) and transverse direction (TD). The true stress-true strain curves of the alloy in RD and TD at different strain rates are shown in Figure 1a-b. It is observed that tensile properties of the material have no significant difference in RD and TD at constant strain rate, which confirms the isotropy of the material after annealing. The true stress-true strain curves at different strains rates are similar also. This is due to the negligible strain rate sensitivity (m)

of the alloy at room temperature: m calculated from Equations (1–2) is about 0.033 in TD and 0.040 in RD. Because of the negligible strain rate sensitivity of AA1050 at room temperature, feed rate and rotational speed of the tool have not been studied in this paper.

$$\sigma = C(\dot{\varepsilon})^m \,|s,T \tag{1}$$

$$m = \left(\frac{d\log\sigma}{d\log\dot{\varepsilon}}\right) \approx \left(\frac{\Delta\log\sigma}{\Delta\log\dot{\varepsilon}}\right)_{s,T} = \frac{\log\sigma_2 - \log\sigma_1}{\log\dot{\varepsilon}_2 - \log\dot{\varepsilon}_1} = \frac{\log\frac{\sigma_2}{\sigma_1}}{\log\frac{\dot{\varepsilon}_2}{\dot{\varepsilon}_1}} \tag{2}$$

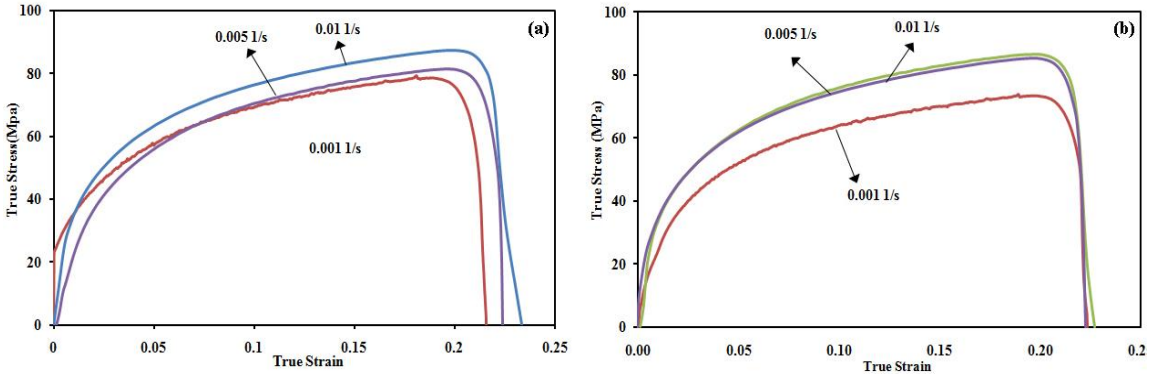

Fig. 1. The true σ-ε curve at different strain rates: a) rolling direction; b) transverse direction

The characteristic parameters of the stress–strain curve, enabling plastic behaviour to be described following power law: $\sigma=143\varepsilon^{0.28}$, are evaluated. Sheet properties are shown in Table 1 according to tensile test at $\dot{\varepsilon}$=0.01 1/s and TD direction.

Table 1. AA1050 sheet properties at ε̇=0.01 1/s and TD direction.

t (mm)	1
E (GPa)	69
Y (MPa)	28
UTS (MPa)	86
El (%)	0.22

FEM modelling of the SPIF process was carried out by means of the ABAQUS/Explicit software, which is able to solve highly non-linear problems. The studied part was a 60° wall angle square-based pyramid with a depth of 23 mm (Fig. 2a). An AA1050 sheet with a size of 200 mm×200 mm×1 mm was considered. Material parameters were obtained from the tensile tests. The mesh size, obtained with trial and error, was finer (2.5 mm) at the centre and larger at the margins of the sheet (Fig. 2b) The tool was considered as a rigid body and its boundary condition was given by the trajectory obtained from CATIA V5R18 software. For verification of simulation results, experimental tests were carried out in a VMC850-CNC milling machine. The geometry described above for process modelling was formed using the same process parameters for the purpose of comparison. In order to evaluate the geometrical accuracy of the produced parts, the surface profiles obtained with the performed tests were measured using a video measuring system (VMS). A micrometre screw gauge was used to make a thickness measurement of the sheet with a precision of 0.01 mm.

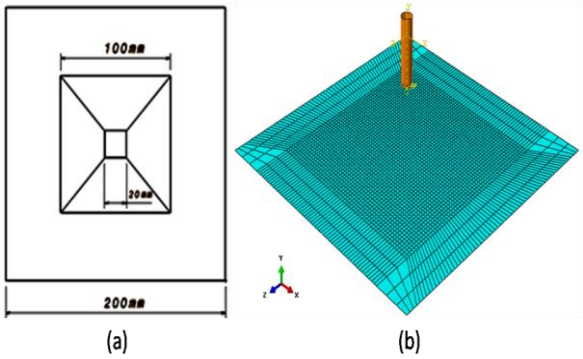

Fig. 2. a) Dimensions of the studied part; b) Model of the forming tool and meshed sheet

The tests were designed based on full factorial design. The studied factors and their levels are shown in Table 2. Figure 3 shows the 10 mm diameter tool in the ABAQUS simulation and experimental test.

Table 2. The studied factors and their levels

Process factor	Level 1	Level 2	Level 3
Tool diameter (D)	5 mm	10 mm	15 mm
Vertical step size (S)	1 mm	1.5 mm	2 mm
Friction coefficient (μ)	0.05	0.1	0.15

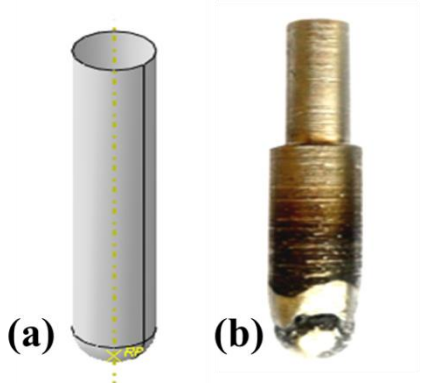

Fig. 3. A 10 mm diameter tool in a) ABAQUS simulation, b) experimental test

After 27 (3^3) runs the vertical force of the tool, minimum thickness of the sheet, and spring-back value were obtained from the software. As in the Rauch et al. study [13], the average of the depth errors of 12 marked points at Figure 4 was considered the spring-back value.

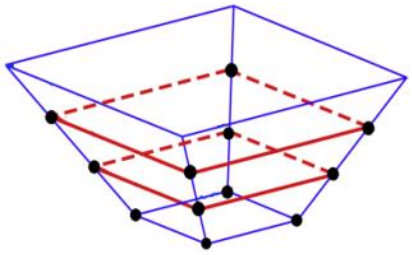

Fig. 4. Marked points to measure the spring-back value

To relate between input and output factors, a back-propagation artificial neural network was designed with a neural network toolbox using MATLAB R2008a software. Nineteen randomly selected datasets (70%) were used to train the neural networks and the remaining eight datasets (30%) were employed to test and verify the network. The ANN models were trained with different numbers of hidden layers and neurons in each layer using the LM algorithm. After training and testing more than 100 networks, the best ANN model for output factors was developed. MSE was taken as the network performance function, which measures the network's performance according to the mean of squared errors (Eq. 3).

$$MSE = \frac{1}{N}\sum_{i=1}^{N}(e_i)^2 = \frac{1}{N}\sum_{i=1}^{N}(t_i - a_i)^2 \qquad (3)$$

where N is the total number of training dataset; t_i is the training sample data and a_i is the output of the neural network [11]. Finally, the trained neural network was defined as the fitness function for GA optimization. The optimum values of D, S, and μ can be efficiently obtained by formulating the optimization problem in a genetic algorithm toolbox using MATLAB R2008a software.

3. Results and Discussion

In order to validate the numerical simulation model, experimental tests were performed and compared with numerical results. For better clarity of the paper, the results of one experimental test are presented (μ=0.05, D=15 mm and S=1.5 mm) (Fig. 5).

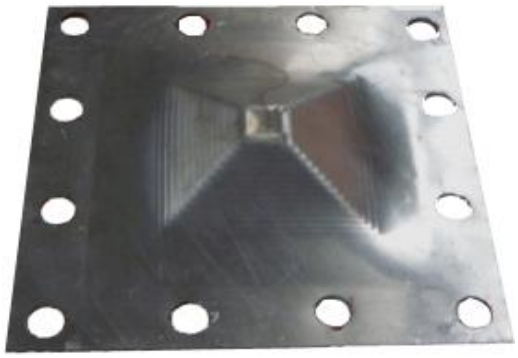

Fig. 5. The produced part at μ=0.05, D=15 mm and S=1.5 mm

3.1. Thickness measurements

Figure 6a shows thickness distribution of the part in the above conditions. The minimum thickness of the sheet is 0.8308 mm at the part's edges and its area increases with the depth of part. Therefore, the thickness of the edges can be considered to be a control factor of part depth. A thickness analysis was carried out to verify the FEM results: the thickness was measured by means of a micrometre with a step of about 4 mm along the X direction. Figure 6b shows the results obtained by thickness measurements with the FEM model,

in comparison with experimental results obtained by testing in the CNC machine. As can be noticed in Figure 6b, thickness values predicted by the FEM method are very close to values measured experimentally. Error values are sufficiently low for the FE to be a useful method for the process design of the incremental sheet metal forming process.

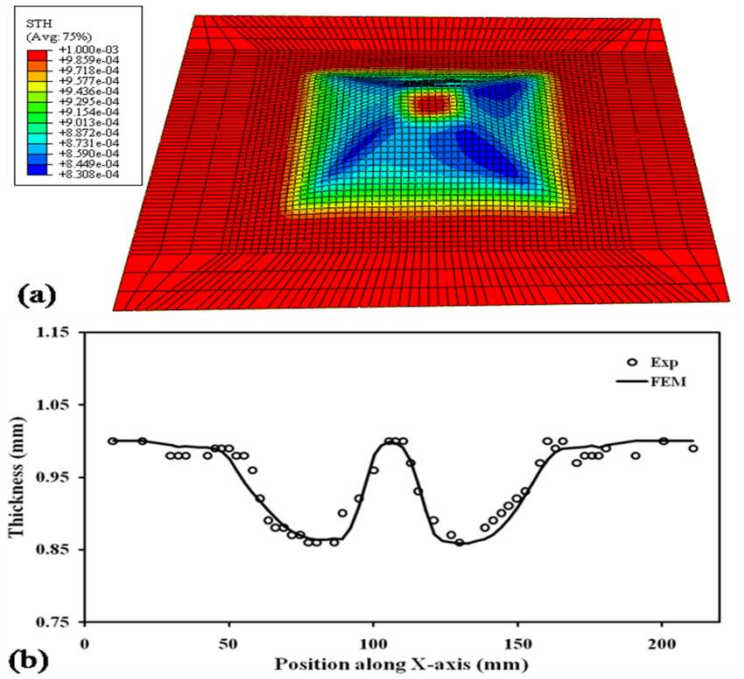

Fig. 6. a) Thickness distribution of the part; b) Thickness comparison between simulation and experiment at μ=0.05, D=15 mm and S=1.5 mm

3.2. Geometrical accuracy

The video measuring system (VMS) was used to evaluate the dimensional accuracy of the deformed sheets. Figure 7 relates the comparison between the original profile defined through a CAD system (theoretical profile), the one obtained through SPIF experiments (experimental profile), and the one resulting from FE simulations (numerical profile). The results indicate that the predicted profile based on the FEM model is very close to the experimental results. Therefore the proposed FEM model can be efficiently utilized to predict the part shape with reasonable accuracy and reliability.

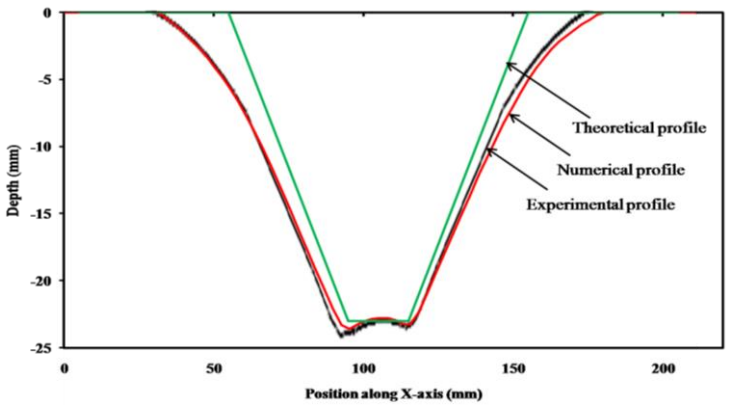

Fig. 7. Comparison between theoretical, numerical, and experimental profile measurements at μ=0.05, D=15 mm and S=1.5 mm

3.3. Force trend

Figure 8 shows a time plot of force at μ=0.05, D=15 mm and S=1.5 mm (F_y is vertical force). The shape of this curve is similar in all 27 runs. A typical force curve starts at zero once forming is initiated. As the tool pushes deeper into the metal, the force quickly increases until a depth is reached where the forces tend to remain approximately constant. Similar behaviour was previously reported for sheet metals by Duflou et al. [7] and Jackson et al. [14]. This is due to dynamic equilibrium between sheet thinning and material strain hardening [5]. Experimental measurement of vertical force was not possible in this study. However, Cerro et al. [9] studied the incremental sheet forming process of 1050 aluminium alloy theoretically and experimentally.

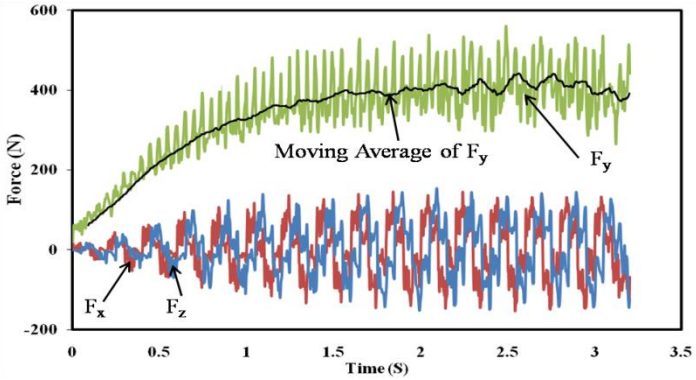

Fig. 8. Forming force trend for μ=0.05, D=15 mm and S=1.5 mm

3.4. FEM Results

The simulated results of vertical force, minimum thickness of the sheet, and spring-back value are shown in Table 3. The min/max of vertical force, minimum thickness of the sheet, and spring-back value is 297/481 N, 0.8147/0.8407 mm and 0.1275/0.1901 mm, respectively.

Table 3. The results of simulation tests

Run	Friction Coefficient	Tool Diameter (mm)	Vertical Step Size (mm)	Min of Thickness (mm)	Vertical Force (N)	Spring-Back (mm)
1	0.05	5	1	0.8395	301	0.1425
2	0.05	5	1.5	0.8365	398	0.1355
3	0.05	5	2	0.8260	415	0.1315
4	0.05	10	1	0.8400	379	0.1615
5	0.05	10	1.5	0.8331	423	0.1528
6	0.05	10	2	0.8221	442	0.1392
7	0.05	15	1	0.8398	407	0.1901
8	0.05	15	1.5	0.8308	445	0.1760
9	0.05	15	2	0.8147	481	0.1415
10	0.1	5	1	0.8402	300	0.1450
11	0.1	5	1.5	0.8357	400	0.1351
12	0.1	5	2	0.8260	411	0.1275
13	0.1	10	1	0.8405	377	0.1619
14	0.1	10	1.5	0.8330	420	0.1454
15	0.1	10	2	0.8228	439	0.1440
16	0.1	15	1	0.8395	405	0.1837
17	0.1	15	1.5	0.8307	442	0.1611
18	0.1	15	2	0.8153	479	0.1459
19	0.15	5	1	0.8402	297	0.1358
20	0.15	5	1.5	0.8340	396	0.1317
21	0.15	5	2	0.8256	408	0.1277
22	0.15	10	1	0.8407	375	0.1548
23	0.15	10	1.5	0.8318	418	0.1453
24	0.15	10	2	0.8238	437	0.1358
25	0.15	15	1	0.8387	403	0.1630
26	0.15	15	1.5	0.8307	439	0.1540
27	0.15	15	2	0.8161	475	0.1464

3.5. ANN Results

The best ANN architecture that would present the predictions is shown in Figure 9. To determine the number of neurons in the hidden layer, several trains are repeated. It is found that a network with one hidden layer consisting of ten hidden neurons produces the best performance. A tangent sigmoid transfer function is used as the activation function for the hidden layer, whereas the linear transfer function can be used for output layer.

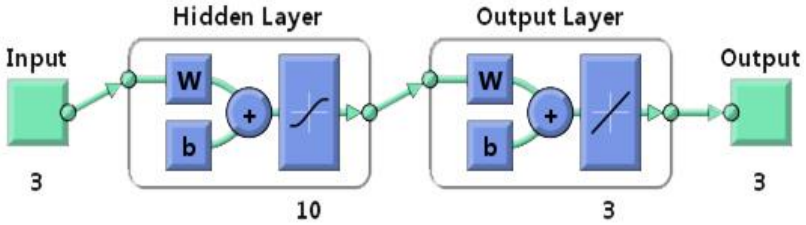

Fig. 9. The optimum architecture of ANN method found for the present study

This network is a kind of feed-forward back-propagation network trained with a Levenberg-Marquardt (LM) algorithm. This algorithm appears to be the fastest method for training moderate-sized feed-forward neural networks [11]. The comparison between the finite element and predicted results by the proposed ANN model is shown in Figure 10a-c. The high values of R and aggregation of data near the ideal 45° line, indicate acceptable network training. The maximum of absolute relative errors are 4.61%, 0.93%, and 10.85% for vertical force, minimum thickness of the sheet, and spring-back value respectively, which are reasonable values for validation of network training.

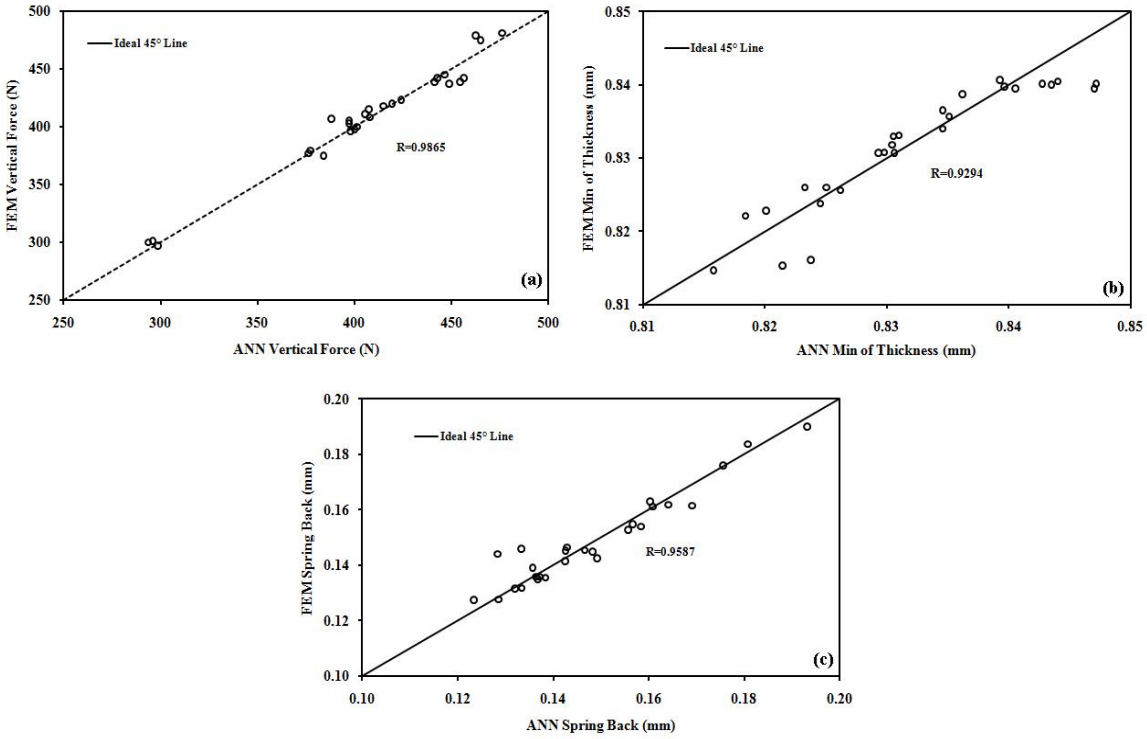

Fig. 10. Comparisons between FEM and ANN date a) Vertical force; b) Minimum thickness of sheet; c) Spring-back

3.5.1. Friction Coefficient Effect

Figure 11a-b indicates the effect of friction coefficient on the minimum thickness of the sheet and on spring-back value, respectively. As can be seen, the friction coefficient has no significant effect on the minimum thickness of

the sheet. Petek et al. [6] reported that lubrication does not influence the force at SPIF of steel DC05. Studies of other sheet metal forming processes have reported different conclusions about the effect of friction coefficient on spring-back value. Papeleux and Ponthot [15] found spring-back vs. friction coefficient curves to exhibit an extremum point. Carden and Geng [16] also reported that the friction coefficient has little effect on spring-back, although very low friction conditions increase spring-back of 6022-T4. Figure 10b shows that an increase in friction coefficient leads to a decrease in spring-back at SPIF of 1050 aluminium alloy.

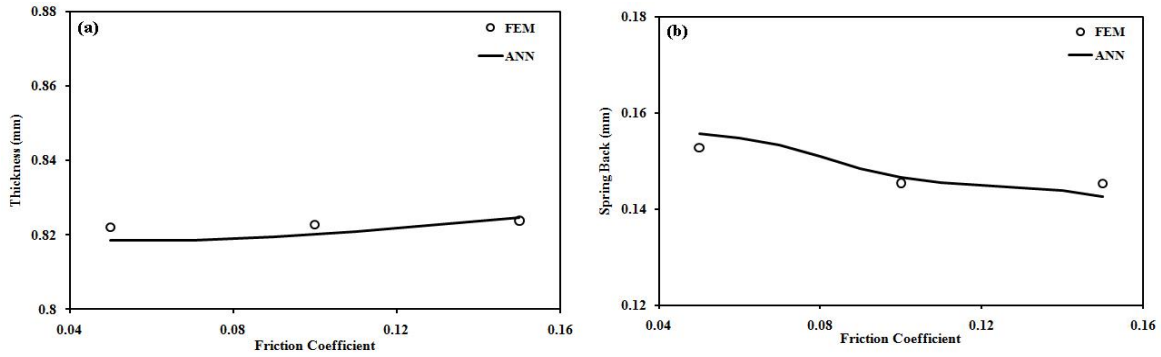

Fig. 11. The effect of friction coefficient on a) Min thickness of sheet at D=10 mm and S=2 mm; b) Spring-back at D=10 and S=1.5 mm

3.5.2. Vertical Step Size Effect

Figures 12a-b indicates the effect of vertical step size on the vertical force and minimum thickness of the sheet respectively. As the vertical step size increases it is apparent that vertical force also rises, which is fully consistent with the results of Petek et al. [6] and Daflou et al. [7]. Petek reported that the magnitude of force at SPIF of steel DC05 is directly proportional to the size of the vertical step, and matches well to linear trend. Daflou reported similar results in the Al3003-O ISMF process. An increase of vertical step size also reduces the minimum thickness of the sheet (Fig. 12b). Growth of vertical force increases the tensile force and sheet thinning overcomes strain hardening, so that the minimum thickness of the sheet is reduced.

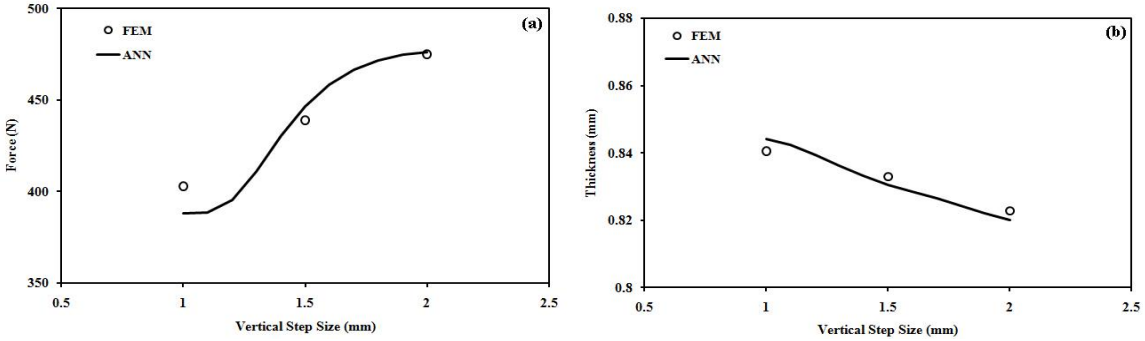

Fig. 12. The effect of vertical step size on a) vertical force at μ=0.15 and D=15 mm; b) Min thickness of sheet at μ=0.1 and D=10 mm

3.5.3. Tool Diameter Effect

Similar to the step size, an increase in tool diameter also causes an increase in the force required for forming (Fig. 13a), which is fully consistent with the results of Petek et al. [6] and Daflou et al. [7]. This is due to a larger contact surface between the tool and the part, which is connected with an increase in the forming force required. Tool diameter increase has no significant effect on the minimum thickness of the sheet whereas it increases spring-back value (Fig. 13b-c).

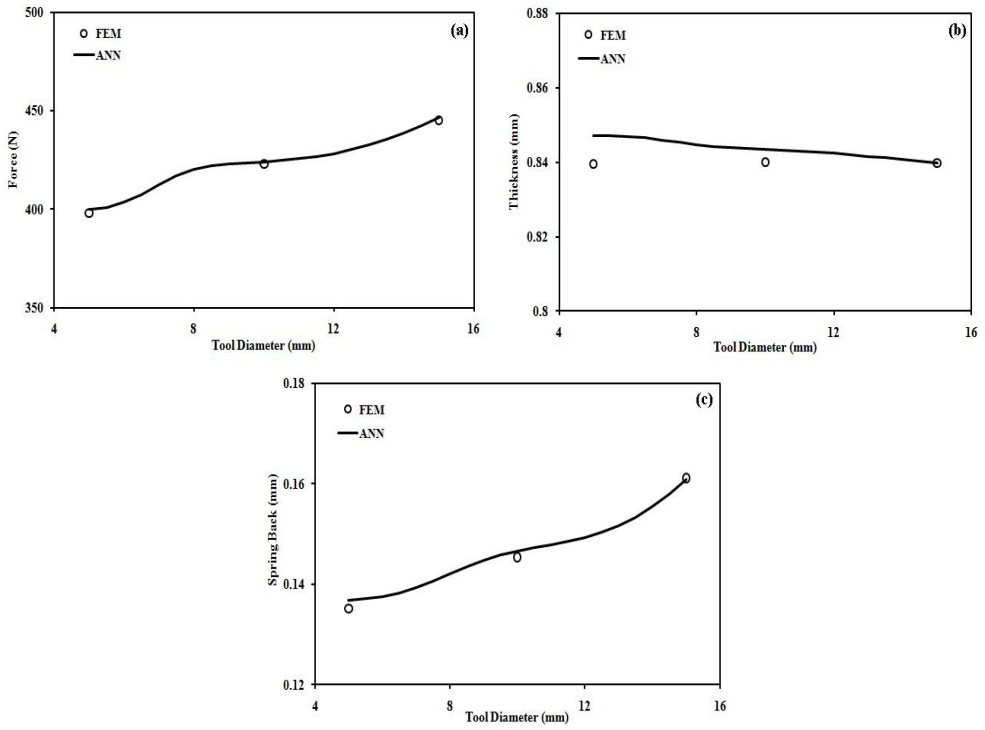

Fig. 13. The effect of tool diameter on a) vertical force at μ=0.05 and S=1.5 mm; b) Min of thickness at μ=0.05 and S=1mm; c) spring-back at μ=0.1 and S=1.5 mm

3.6. Optimization Results

In order to find optimum values of friction coefficient, tool diameter and vertical step size to get minimum vertical force and spring-back value and maximum value of minimum thickness of the sheet, the trained neural network is defined as the fitness function for GA optimization. In this study, a population size of 200, crossover fraction of 0.8, mutation rate of 0.01 and number of generations of 2000 are employed. Rank scaling function, stochastic uniform selection function, elite count reproduction function, and Gaussian mutation function are adopted as the GA options. Solution of a multi-objective optimization creates a set of optimum points called Pareto front (Fig. 14). These points are optimal values of the vertical force, spring-back, and minimum thickness of the sheet. Because the GA can only minimize the objective functions, 'maximizing of min thickness' is replaced with 'minimizing of (-) min thickness', so values of thickness are negative. As can be seen from Figure 14, some regions of the Pareto front are empty. Evaluation of optimum points at the last generation of the GA algorithm shows that vertical force values of some points can be placed in the empty regions, but when sorting and ranking the optimum points, these points have not been placed at the Pareto front, so some regions of the front appear empty. The utopia point is obtained by minimizing each objective function without regard for other objective functions. The minimum vertical force is 278.52N (at μ=0.15, D=5 mm and S=1.13 mm), the maximum value of minimum thickness is 0.8424 mm (at μ=0.15, D=5 mm and S=1.17 mm) and the minimum spring-back value is 0.1119 mm (at μ=0.15, D=5 mm and S=1.87 mm), so the utopia point is located at (278.52, -0.8424, 0.1119). It is observed that μ=0.15 and D=5 mm are optimum values at all objective functions. A special point of the Pareto front is the one at the minimum distance from the utopia point: this point is located at (302.7, -0.8393, 0.1301) with a friction coefficient of 0.05, tool diameter of 5 mm, and vertical step size of 1.31 mm (0.05, 5,1.31).

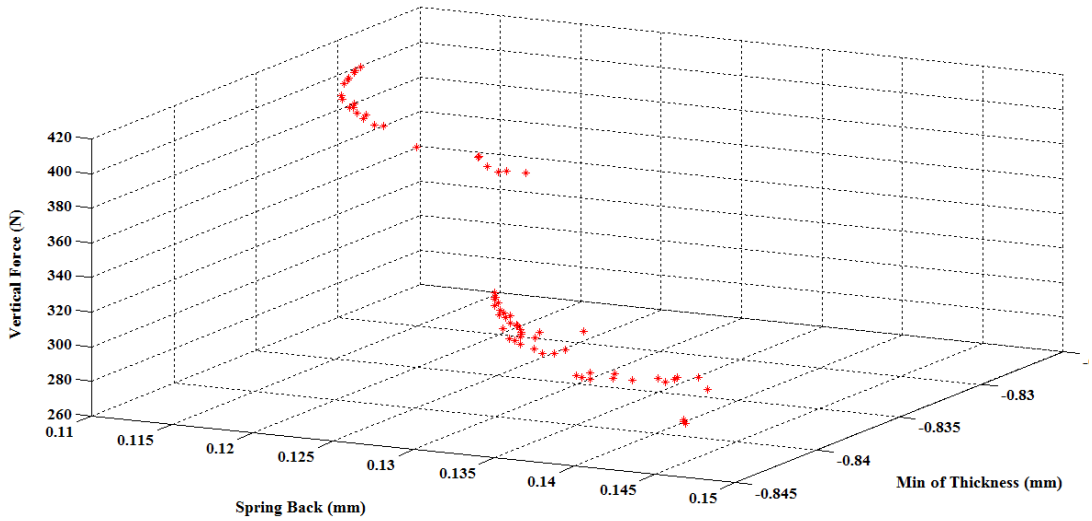

Fig. 14. The Pareto front calculated with GA

4. Conclusions

The results of simulation tests, trained neural network, and optimum values for process parameters are summarized as follows:

1. A back-propagation neural network model can predict an accurate relationship between SPIF input factors and output results.

2. Genetic algorithm is a suitable tool for the optimization of process factors to minimize vertical force and spring-back values and maximize the minimum thickness of the sheet.

3. The proposed method of optimization showed that D=5 mm and μ=0.015 are optimum values of tool diameter and friction coefficient for each objective function, whereas vertical step size takes different values for optimizing the functions.

References

[1].Dejardin S., Thibaud S., Gelin J.C., Michel G., 2010, Experimental investigations and numerical analysis for improving knowledge of incremental sheet forming process for sheet metal parts, J. Mater. Process. Tech. **210**: 363-369.

[2].Leszak E., 1967, Apparatus and Process for Incremental Dieless Forming, Patent US3342051A1.

[3].Micari F., Ambrogio G., Filice L., 2007, Shape and dimensional accuracy in single point incremental forming: State of the art and future trends, J. Mater. Process. Tech. **191**(1-3): 390–395.

[4].Kim Y.H., Park J.J., 2002, Effect of process parameters on formability in incremental forming of sheet metal, J. Mater. Process. Tech. **130**(1): 42-46.

[5].Durante M., Formisano A., Langella A., Memola Capece Minutolo F., 2009, The influence of tool rotation on an incremental forming process, J. Mater. Process. Tech. **209**: 4621-4626.

[6].Petek A., Kuzman K., Kopač J., 2009, Deformations and forces analysis of single point incremental sheet metal forming, Arch. Mater. Sci. and. Eng. **35**: 107-116.

[7].Duflou J., Tunckol Y., Szekeres A., Vanherck P., 2007, Experimental study on force measurements for single point incremental forming, J. Mater. Process. Tech. **189**: 65-72.

[8].Henrard C. , Bouffioux C. , Eyckens P. , Sol H. , Duflou J. R. , Van Houtte P. , Van Bael A. , Duchêne L. , Habraken A. M. ,2011, Forming forces in single point incremental forming: prediction by finite element simulations, validation and sensitivity, Computational Mechanics **47**: 573-590.

[9].Cerro I., Maidagan E., Arana J., Rivero A., Rodr´ıguez P.P., 2006, Theoretical and experimental analysis of the dieless incremental sheet forming process, J. Mater. Process. Tech. **177**: 404-408.

[10]. Sanjari M., Karimi Taheri A., Movahedi M.R., An optimization method for radial forging process using ANN and Taguchi method, Int. J. Adv. Manuf. Technol. **40**: 776-784.

[11]. Min Y. Yu, W., Hai-bo W., Lin H., 2010, Optimization of press bend forming path of

aircraft integral panel, T. Nonferr. Metal. Soc. **20**: 294-301.

[12]. Lopes A.B., Barlat F., Gracio J.J., Ferreira Duarte J.F., 2003, Effect of texture and microstructure on strain hardening anisotropy for aluminum deformed in uniaxial tension and simple shear, Int. J. of Plasticity. **19**: 1-22.

[13]. Rauch M., Hascoet J.Y., Hamann J.C., Plenel Y., 2009, Tool path programming optimization for incremental sheet forming applications, Comput.-Aided. Des. **41**: 877-885.

[14]. Jackson K.P. , Allwood J.M. , Landert M., 2008, Incremental forming of sandwich panels, J. Mater. Process. Tech. **204**: 290–303.

[15]. Papeleux L., Ponthot J.P., 2002, Finite element simulation of springback in sheet metal forming, J. Mater. Process. Tech. **125-126**: 785-791.

[16]. Carden W.D., Geng L.M., Matlock D.K., Wagoner R.H., 2002, Measurement of Springback, Int. J. Mech. Sci. **44**: 79-101.